Link between Coulomb stress changes and seismic activation in the Marmara sea after the 1999, Izmit (Turkey), earthquake

V. Durand,[1,3] M. Bouchon,[1] H. Karabulut,[2] D. Marsan,[3]

J. Schmittbuhl,[4]

[1]ISTERRE, Universite de Grenoble, Centre National de la Recherche Scientifique, Grenoble, FRANCE

[2]Kandilli Observatory and Earthquake Research Institute, Istanbul, TURKEY

[3]ISTERRE, Universite de Savoie, Le Bourget-du-Lac, FRANCE

[4]Institut de Physique du Globe de Strasbourg, Universite de Strasbourg, Centre National de la Recherche Scientifique, Strasbourg, FRANCE

Abstract. We investigate the effect of dynamic and static stress changes produced by the 1999 Izmit earthquake, on four pre-existing seismic clusters located in the eastern Marmara sea, beyond the western termination of the earthquake rupture. These four clusters show long-lasting modifications in their seismicity rate. We observe that these seismic activity variations are related to stress changes. Dynamic stress pulses activate strike-slip faulting instantaneously but, in the absence of a concomitant static Coulomb stress increase, this activation is short lived. Indeed, a large dynamic stress combined with a negative static Coulomb stress may result in an immediate activation followed by the occurrence of a seismicity shadow. In contrast, the activation of extensional clusters begins slowly and takes a few days to fully develop. It is also remarkably long-lasting and does not follow a classical Omori decay. More than 10 years after the earthquake, the extensional clusters located near the termination of the rupture, where static stress and pressure changes were high, are still activated.

1. Introduction

It is now well established that stress changes induced by large earthquakes can affect seismicity at close and far distances (*Das and Scholz*, [1981]; *Stein and Lisowski*, [1983]; *Reasenberg and Simpson*, [1992]; *Hill et al.*, [1993]; *Anderson et al.*, [1994]; *Bodin and Gomberg*, [1994]; *King et al.*, [1994]; *Harris*, [1998]; *Brodsky et al.*, [2000]; *Gomberg et al.*, [2001, 2004]; *Marsan*, [2003]; *Prejean et al.*, [2004]; *Steacy et al.*, [2005]; *Daniel et al.*, [2006]; *Hill and Prejean*, [2007]) and may trigger or modify the timing of future earthquakes in the region (*Harris and Simpson*, [1992]; *Stein et al*, [1992, 1999]; *Nalbant et al*, [1998]; *Toda et al.*, [1998]; *Cocco et al*, [2000]). On the North Anatolian Fault (NAF), a combination of static Coulomb stress increases on neighboring fault segments (*Stein et al.*, [1997]) and long-range dynamic stress excitation of extensional seismic clusters (*Durand et al.*, [2010]) explains the migration of large ruptures along this major plate boundary (*Toksöz et al.*, [1979]). However, an understanding of the deformation mechanisms which are set in action by permanent or transient stress changes is lacking and requires more detailed observations. The aim of this study is to add a set of observations based on the long-term monitoring of seismicity in the eastern Marmara sea, a region which was strongly shaken by the 1999 Mw 7.6 Izmit earthquake. This region is of particular interest because of the possible nucleation there of the next large earthquake in the NAF sequence.

Previous calculations of static stress increase on faults in this region after the Izmit earthquake have been performed by *Parsons et al.*, [2000] to infer probabilistic seismic risk for Istanbul and by *Çakir et al.*, [2003a]. In the present study we investigate the

link between stress and seismicity changes and we try to separate the roles of static and dynamic stimulations.

2. Faults and Seismicity in the Region

The Izmit earthquake occurred on August 17, 1999 and ruptured the east-west running North Anatolian Fault bilaterally over a length of about 150km (*Barka et al.*, [2002]; *Çakir et al.*, [2003b]). Nearly three months later, on November 12, the Mw 7.2 Düzce earthquake extended the rupture 40km eastward. To the west, the rupture ended in the Cinarcik basin, where the main branch of the NAF abruptely changes direction and is referred to as the Main Marmara Fault (MMF) (*Le Pichon et al.*, [2001]). The seismic activity in the eastern Marmara sea following the earthquake is depicted in Figure 1a. This figure displays seismic events which occurred between August 17 and November 5, 1999 when many seismic stations were deployed in the region (*Karabulut et al.*, [2011]). We shall use the corresponding relocated catalog for this period and the national turkish catalog of the Kandilli Observatory (Figure 1b) for the decade before and after the earthquake to study the evolution of activity in the region and to investigate its relation to stress changes. Besides the concentration of seismicity along the earthquake rupture, the post-Izmit activity clusters in a few areas: The Prince's Islands zone of the MMF, the area off the Tuzla peninsula just north of the termination of the Izmit rupture, the Yalova region to the southwest of the rupture termination, and, further south, the Gemlik region around the Middle Branch of the NAF. This activity takes place in two major types of seismic events: Strike-slip events which are associated with the NAF system, and normal faulting events associated with the aegean extension. A cut-off magnitude is utilized to select the earthquakes used in the following analysis. We selected M$\geq$ 2.8

for the Tuzla and Yalova areas, and M$\geq$ 3.0 for the Prince's Islands and Gemlik zones. These cut-off magnitudes were chosen after computing the frequency-magnitude curves for each zone, and making sure that it follows a Gutemberg-Richter law for M$\geq$Mc. Except for Prince's Islands, where the limited number of earthquakes (only 31 events of magnitude above or equal to 3.0) prevented us to do so, we observed no significant rupture from a Gutemberg-Richter law down to cut-off magnitude, for separate time intervals (01/01/1989-08/16/1999, 08/17/1999-12/31/2001, 01/01/2002-08/17/2009) for each zone.

3. Observations

3.1. Prince's Islands

The Prince's Islands cluster is located on the Main Marmara Fault, the continuation of the main branch of the NAF in the Marmara sea (Figure 1). Only the relocated data are used here, since the unrelocated (Kandilli) catalog does not allow to select earthquakes in this case (see figure 1). As a consequence, we could not estimate the rate of earthquakes in this cluster prior to the Izmit mainshock. The evolution of seismic activity in this cluster is shown in Figure 2a. It is characterized by a strong immediate activation followed by a rapid extinction of the activity. Indeed, some of the largest early aftershocks of the earthquake occurred in this cluster (*Orgülü and Aktar*, [2001]; *Ozalaybey et al.*, [2002]). These events have almost pure strike-slip mechanism with a nodal plane oriented along the fault direction (*Orgülü and Aktar*, [2001]; *Ozalaybey et al.*, [2002]). The Coulomb stress produced by the earthquake on the MMF at the center of this cluster and near its medium depth (Table 1) is shown in Figure 2b. The stress is calculated using the fault model inferred for the earthquake (*Bouchon et al.*, [2002]) and the discrete wavenumber

method (*Bouchon*, [1981]; *Cotton and Coutant*, [1997]). A friction coefficient of 0.6 is assumed. Other values (0.4 to 0.7) were also tested. The influence of this corfficient is very limited (figure 2b). While the static Coulomb stress increase is relatively small (a little over 1 bar), the positive peak of the dynamic Coulomb stress reaches about 28 bars, a value typical of what is often observed for earthquake stress drops. In view of Figures 2a,b, we interpret the immediate and strong activation of this short segment of the NAF as triggered by the high dynamic stress pulse radiated by the earthquake. Likewise, we attribute its rapid extinction to the low level of the permanent Coulomb stress increase. These observations support the view that static stress changes and transient deformations have different timescales as it has been proposed (*Marsan*, [2003]; *Voisin et al.*, [2004]).

3.2. Gemlik (Middle branch)

Seismicity on and around the Middle Branch of the NAF is clearly activated by the Izmit earthquake near the place where the Middle Branch enters the Marmara sea (Figure 1). The length of the fault segment which is activated is relatively long and extends over about 50 km. Background seismic activity in the region shows that this zone encompasses both strike-slip and normal faulting events (*Karabulut et al.*, [2011]). Normal faulting events dominate onshore, whereas strike-slip events tend to occur offshore. The activation is immediate offshore where the strike-slip regime dominates, while it takes a few days to develop onshore, reaching its peak there about a week after the earthquake (Figure 1a). The activation lasts for several months and is followed by an almost total extinction which lasts for nearly two years (Figure 3a).

We compute the rate of background earthquakes prior to and posterior to the Izmit earthquake. Background earthquakes are those events that remain after declustering, so that

their rate can directly be interpreted as a forcing rate alone in the absence of any earthquake interactions. We here compute the background rate using the simple approach of *Hainzl et al.*, [2006], which is appropriate at these long time scales. For the Gemlik area, the background rate after the Izmit earthquake (0.0070 events per day) is nearly three times smaller than the one before (0.0130 events per day).

The Coulomb stress calculated for a fault orientation and mechanism representative of the Middle Branch of the NAF (Table 1, Figure 3b) reaches a positive dynamic value of about 8 bars but has a negative static value of 4±0.5 bars (depending on the value of the friction coefficient). Nearly similar values are obtained for the normal faulting events geometry. Thus, like what is observed on the Prince's Islands segment of the MMF, the dynamic stress seems to control the seismicity at short time range (immediate activation), whereas the static stress could control its long time range evolution (decrease of seismic rate and seismicity shadow). The migration of seismicity from offshore to onshore after a few days suggests a rapid decrease of the strike-slip activity, as observed along the MMF, and a slow decrease of normal-fault activity. The emergence of quiescence after a period of triggered activity has been observed elsewhere (*Marsan*, [2003]; *Ma et al.*, [2005]; *Marsan and Nalbant*, [2005]; *Daniel et al.*, [2008]). Like in the present case, these observations show short term triggering followed by long term quiescence, suggesting the existence of two distinct interaction regimes, a first one caused by the destabilisation of active faults by travelling seismic waves, and a second one due to the remaining static stress perturbation (*Marsan and Nalbant*, [2005]).

3.3. Tuzla cluster

This cluster is of particular interest because it lays near the junction of the Izmit rupture with the Main Marmara Fault. If static Coulomb stress increase alone were to determine the nucleation site of the next large earthquake on the NAF, it is logically where it would happen. Most of the events in this cluster have normal faulting mechanisms and are located between depths of 5 and 10km (*Karabulut et al.*, [2002]). The evolution of seismicity (Figure 4a) shows a strong activation following the Izmit earthquake. Like for the normal faulting events around the Middle Branch of the NAF, this activation was not immediate but built up slowly over several days and reached its peak about a week after the earthquake (*Durand et al.*, [2010]). This slow onset suggests that fluids could be responsible of the activation of seismicity. This activation does not appear limited in time, as 10 years after the earthquake the background activity (0.0064 events per day) is still higher than what it was before (0.0017 events per day). The normal faults in this area underwent a peak dynamic Coulomb stress of about 30 bars during the earthquake and have had a permanent Coulomb stress increase of nearly 9±2 bars ever since (Figure 4b), depending on the value of the friction coefficient.

3.4. Yalova cluster

This cluster is a long-recognized nest of seismicity located southwest of the termination of the Izmit rupture. It covers an area about 20km across which is well known for its geothermal springs. It was strongly activated by the Izmit earthquake and is made up of normal faulting events on north-dipping east-west trending faults (*Karabulut et al.*, [2002]; *Ozalaybey et al.*, [2002]; *Bulut and Aktar*, [2007]). Like for the other normal faulting events in the region, the seismic activity was not immediate but built up slowly over a few

days (*Daniel et al.*, [2006]; *Durand et al.*, [2010]). As shown in Figure 5a, 10 years after the earthquake, the background rate (0.0250 events per day) is still considerably higher than what it was before (0.0061 events per day). The Coulomb calculation shows a large negative static value (-6 ±1 bars) on the normal faults in the area (Figure 5b), while the positive peak of the dynamic stress is relatively small. Thus, the strong activation of long duration which is observed is not related to Coulomb stress. A calculation of the pressure produced by the earthquake at the center of the cluster (Figure 6) shows that the area underwent a permanent compression of about 11 bars. The reaction of the fluid-filled fractured area to this high pressure increase seems the logical mechanism of the activation.

4. Discussion

In order to gain more insight into the link between stress and seismicity, we calculate the spatial variation of the Coulomb stress in the eastern Marmara sea. To do so, we separate the different tectonic regimes of the region into 6 zones, which cover the areas where known faults or seismic activity are present (Table 2). In each zone we consider the predominant fault orientation and mechanism associated with the seismicity and evaluate the corresponding Coulomb stress at a grid of points located at 5km interval and 10km depth. The resulting map of the positive peak of the dynamic Coulomb stress is presented in Figure 7. The seismicity which occurred in the day following the earthquake is superposed on the stress map. The largest events in the region on this day are associated with the two branches of the NAF: the Prince's Islands segment of the MMF, and the Gemlik Bay segment of the Middle Branch of the NAF. These events are located in areas where the dynamic Coulomb stress is particularly high. On the Middle Branch

the seismicity is only observed on the offshore segment where the dynamic stress is the highest. The inland segment, closer to the Izmit rupture but where the dynamic stress is significantly lower seems devoid of activity. This suggests that the activation along the Middle Branch is controlled by the directivity of the Izmit rupture, as has been observed elsewhere (*Gomberg et al.*, [2001, 2003]). A similar calculation done for a normal faulting mechanism in this zone instead of a strike-slip one, is presented in Supplementary Figure S1. It shows a lower value of the dynamic stress in this zone. This indicates that the dynamic Coulomb stress around the Middle Branch is more likely to have triggered strike-slip rather than normal-faulting events, in agreement with what is observed on the day after the earthquake.

The map of static Coulomb stress is presented in Figure 8. Its value is inferred from the level of the stress time history 100s after the start of the earthquake. As seen in Figures 2b-5b, the stress has by then reached its permanent value. The seismicity which occurred between October 1st (6 weeks after the earthquake) and November 5th, 1999 is superposed on the map. Most of the seismic activity which occurs away from the Izmit rupture is now associated with normal-faulting events. To the north of the rupture termination, the Tuzla cluster location correlates with an area of large static stress. In contrast, activity on the Prince's Islands section of the MMF where the static stress is low (about 1 bar) is now almost extinct. To the south, seismic activity has picked up in the inland and coastal area around Gemlik, where normal faulting dominates, but has largely decreased on the offshore segment of the Middle Branch of the NAF. The rapid decrease of strike-slip activity there and in Prince's Islands correlates with negative or low values of the static Coulomb stress on the associated strike-slip faults. The strongest

193 activation in the weeks and months following the earthquake occurs in the Yalova cluster.
194 This activation is in the form of normal faulting events and, like the activation of normal
195 faulting events in the Gemlik area (Supplementary Figure S2), it corresponds to a zone
196 of decrease in static Coulomb stress. The main reason for the negative static Coulomb
197 stress at Yalova and Gemlik is that these zones are put under compression after the Izmit
198 earthquake. This has the effect of increasing the normal stress (in absolute value) across
199 faults and, in the absence of fluids, would increase friction. The two areas, and more
200 particularly Yalova, have been known since antiquity for their geothermal springs which
201 are present throughout the region (*Eisonlohr*, [1996]). This indicates the widespread
202 presence of crustal fluids circulating in this highly fractured region. The map showing
203 the static pressurization of the region produced by the earthquake is presented in Figure
204 9. The large permanent compression undergone by the Yalova region resulted in a large
205 long-lasting increase of its seismic activity (Figure 5a), which is still being felt more than
206 10 years before the earthquake.

207 The parallel observations of seismicity and stress in the eastern Marmara sea following
208 the Izmit earthquake help shed some light on how stress changes affect seismicity. As
209 emphasized elsewhere (*Dewey*, [1976] ; *Karabulut et al.*, [2011]) the interest of the region
210 is that it combines in the same place intense strike-slip deformation and intense extension.
211 In spite of this apparent complexity, what we observe is surprisingly simple and seems
212 physically logical:

213 1. The strike-slip events are immediately activated after the earthquake. They occur
214 on two sections of the NAF (the MMF and the Middle Branch) which underwent high dy-

namic Coulomb stress and small or negative static Coulomb stress. Thus, their activation seems triggered by the dynamic stress.

2. This strike-slip activity decays very rapidly. The short duration of the dynamic stress excitation that these areas underwent compared to the sustained excitation that static stress would procure seems consistent with a rapid extinction of the activity as observed elsewhere (*Gomberg et al.*, [2001]) and reproduced experimentally (*Belardinelli et al.*, [2003]).

3. Intense normal faulting activity seems triggered by the static deformation of a crustal volume where the presence of fluids is widespread. *Beeler et al.*, [2000] and *Cocco and Rice*, [2002] have shown that fluids can decrease the effective normal stress enough to trigger failure while *Hill and Prejean*, [2007] suggest that fluid-driven deformations are sufficient to trigger events. For the Yalova and Gemlik regions, pressure increase seems to have been the triggering factor. In Tuzla where the presence of crustal fluids is less documented, static Coulomb stress increase or permanent volume dilatation or a combination of both were possible triggers.

4. The normal faulting activity begins slowly and builds up over a few days. Because this activation involves fluid circulation in a large crustal volume, the presence of a period during which the activity builds up and extends spatially (*Karabulut et al.*, [2011]) seems to be expected. *Nur and Booker*, [1972] have shown that the redistribution of the pore pressure by fluid flow can lead to a decrease of the strength of faults and delayed rupture.

5. Once started, the normal faulting activity lasts for a long time. In Yalova and Tuzla the seismicity is still considerably higher more than 10 years after the earthquake than

what it was before. In Gemlik, where the permanent deformation is smaller, the activation lasted for about 10 months.

Combined with other studies, the observations that we have reported show the variety and richness of the seismic triggering mechanisms involved. Transient or static Coulomb stress increases can both activate the same seismogenic structure. Which one dominates in a given case is necessarily a function of the distance to the source of the excitation. For instance, three months after the Izmit earthquake, the Yalova cluster was slightly activated by the Düzce earthquake nearly 200km away, making dynamic stress the likely triggering excitation at that time (*Daniel et al.*, [2006]).

The present observations reinforce the differences which have been previously observed between the response of extensional zones and strike-slip faults (*Hill and Prejean*, [2007]; *Durand et al.*, [2010]). The remarkable sensitivity of extensional clusters to stress excitation which is often seen by the long range triggering of these clusters, is shown here by the very long duration of their activation. Their delayed response shows that the strain changes induced by the earthquake initiate physical processes which take some time to fully develop (*Gomberg*, [1996]; *Freed*, [2005]; *Hill and Prejean*, [2007]). The peak of activation occurs here after a few days, providing an order for the time constant of the processes involved.

The present observations also confirm the limited time efficiency of dynamic triggering previously reported (*Marsan*, [2003]; *Voisin et al.*, [2004]). This characteristic which is displayed here for strike-slip faulting, does not, however, apply to extensional clusters for which fluids may be the triggering agent (*Durand et al.*, [2010]).

Acknowledgments. (Text here)

References

Anderson, J.G., J.N. Brune, J.N. Louie, Y. Zeng, M. Savage, G. Yu, Q. Chen, and D. dePolo (1994), Seismicity in the western Great Basin apparently triggered by the Landers, california, earthquake, 28 June 1992, *Bull. Seism. Soc. Am.*, *84*, 863–891

Barka, A., H. S. Akyüz, E. Altunel, G. Sunal, Z. Cakir, A. Dikbas, B. Yerli, R. Armijo, B. Meyer, J. B. de Chabalier, T. Rockwell, J. R. Dolan, R. Hartleb, T. Dawson, S. Christofferson, A. Tucke, T. Fumal, R. Langridge, H. Stenner, W. Lettis, J. Bachhuber, and W. Page (2002), The surface rupture and slip distribution of the 17 August 1999 Izmit earthquake (M 7.4), North Anatolian fault, *Bull. Seism. Soc. Am.*, *92*, 43–60

Beeler, N. M., R. W. Simpson, D. A. Lockner, and S. H. Hickman (2000), Pore fluid pressure, apparent friction and Coulomb failure, *J. Geophys. Res.*, *105*, 25533–25554

Belardinelli, M. E., A. Bizzarri, and M. Cocco (2003), Earthquake triggering by static and dynamic stress changes, *J. Geophys. Res.*, *108*, 2135

Bodin, P., and J. Gomberg (1994), Triggered seismicity and deformation between the Landers, California, and Little Skull Mountain, Nevada, earthquakes, *Bull. Seism. Soc. Am.*, *84*,835–843

Bouchon, M. (1981), A simple method to calculate Green's functions in elastic layered media, *Bull. Seism. Soc. Am.*, *71*,959–971

Bouchon, M., M. N. Toksöz, H. Karabulut, M.-P. Bouin, M. Dietrich, M. Aktar, and M. Edie (2002a), Space and time evolution of rupture and faulting during the 1999 Izmit (Turkey) earthquake, *Bull. Seism. Soc. Am.*, *92*, 256–266

Brodsky, E.E., V. Karakostas, and H. Kanamori (2000), A new observation of dynamically triggered regional seismicity: Earthquakes in Greece following the August 1999

Izmit, Turkey earthquake, *Geophys. Res. Lett.*, *27*, 2741–2744

Bulut, F., and M. Aktar (2007), Accurate relocation of Izmit earthquake (Mw=7.4, 1999) aftershocks in Cinarcik Basin using double difference method, *Geophys. Res. Lett.*, *34*, L10307, doi:10.1029/2007GL029611

Çakir, Z., A. A. Barka, E. Evren (2003a), Coulomb stress interactions and the 1999 Marmara earthquakes, *Turkish J. Earth Sci.*, *12*, 91–103

Çakir, Z., J.B. de Chabalier, R. Armijo, B. Meyer, A.A. Barka, and G. Pelzer (2003b), Seizsmic and early post-seismic slip associated with the 1999 Izmit earthquake (Turkey), from SAR interferometry and tectonic field observations, *Geophys. J. Int.*, *155*, 93–110

Cocco, M., C. Nostro, and G. Ekström (2000), Static stress changes and fault interaction during the 1997 Umbria-Marche earthquake sequence, *J. Seism.*, *4*, 501–516

Cocco, M., and J. R. Rice (2002), Pore pressure and poroelasticity effects in Coulomb stress analysis of earthquake interactions, *J. Geophys. Res.*, *107*

Cotton, F., and O. Coutant (1997), Dynamic stress variations due to shear faults in a plane layered medium, *Geophys. J. Int.*, *128*, 676–688

Daniel, G., D. Marsan, and M. Bouchon (2006), Perturbation of the Izmit earthquake aftershock decaying activity following the 1999 Mw7.2 Düzce, Turkey, earthquake, *J. Geophys. Res.*, *111*, B05310, doi:10.1029/2005JB003978

Daniel, G., D. Marsan, and M. Bouchon (2008), Earthquake triggering in southern Iceland following the June 2000 Ms 6.6 doublet, *J. Geophys. Res.*, *113*, B05310

Das, S., and C.H. Scholz (1981), Off-fault aftershock clusters caused by shear stress increase? *Bull. Seism. Soc. Am.*, *71*, 1669–1675

Dewey, J. W. (1976), Seismicity of northern Anatolia, *Bull. Seism. Soc. Am.*, *66*, 843–868

Durand, V.,M. Bouchon, H. Karabulut, D. Marsan, J. Schmittbuhl, M.-P. Bouin, M. Aktar, and G. Daniel (2010), Seismic interaction and delayed triggering along the North Anatolian Fault, *Geophys. Res. Lett.*, *37*

Eisonlohr, T. (1996), The thermal springs of Armutlu peninsula (NW Turkey) and their relationship to geology and tectonic, *in Schindler, C., Pfister, M. (Eds), Active Tectonics of North-Western Anatolia : The Marmara Poly-Project.*, Cambridge Publications, 197–228 Freed, A.M. (2005), Earthquake triggering by static, dynamic, and postseismic stress transfer, *Ann. Rev. Earth Planet. Sci.*, *33*, 335–367

Gomberg, J. (1996), Stress/strain changes and triggered seismicity following the Mw 7.3 Landers, California, earthquake, *J. Geophys. Res.*, *101*, 751-764

Gomberg, J., P. A. Reasenberg, P. Bodin, and R. A. Harris (2001), Earthquake triggering by seismic waves following the Landers and Hector Mine earthquakes, *Nature*, *411*, 462–466

Gomberg, J., P. Bodin, and P.A. Reasenberg (2003), Observing earthquakes triggered in the near field by dynamic deformations, *Bull. Seism. Soc. Am.*, *93*, 118–138

Gomberg, J., P. Bodin, K. Larson, and H. Dragert (2004), Earthquake nucleation by transient deformations caused by the M=7.9 Denali, Alaska, earthquake, *Nature*, *427*, 621–627

Hainzl, S., F. Scherbaum, and C. Beauval (2006), Estimating background activity based on interevent-time distribution, *Bull. Seism. Soc. Am.*, *96*, 118–138, doi:10.1785/0120050053

Harris, R. A. (1998), Introduction to special section: Stress triggers, stress shadows, and implications for seismic hazard, *J. Geophys. Res.*, *103*, 24347–24358

Harris, R.A., and R.W. Simpson (1992), Changes in static stress on southern California faults after the 1992 Landers earthqueke, *Nature*, *360*, 251–254

Hill, D. P., P. A. Reasenberg, A. Michael, W. J. Arabaz, G. Beroza, D. Brumbaugh, J. N. Brune, R. Castro, S. Davis, D. dePolo, W. L. Ellsworth, J. Gomberg, S. Harmsen, L. House, S. M. Jackson, M. J. S. Johnston, L. Jones, R. Keller, S. Malone, L. Munguia, S. Nava, J. C. Pechmann, A. Sanford, R. W. Simpson, R. B. Smith, M. Stark, M. Stickney, A. Vidal, S. Walter, V. Wong and J. Zollweg (1993), Seismicity remotely triggered by the magnitude 7.3 Landers, California, Earthquake, *Science*, *260*, 1617–1623, doi:10.1126/science.260.5114.1617

Hill, D. P., and S. G. Prejean (2007), Dynamic triggering, *in Treatise on Geophysics* (H. Kanamori, ed.), Vol. *4*, 257-291, Elsevier.

Karabulut, H., M.-P. Bouin, M. Bouchon, M. Dietrich, C. Cornou, and M. Aktar (2002), The seismicity in the eastern Marmara Sea after the August 17, 1999 Izmit earthquake, *Bull. Seism. Soc. Am.*, *92*, 387–393

Karabulut, H., J. Schmittbuhl, S. Özalaybey, O. Lengliné, A. Kömu-Mutlu, V. Durand, M. Bouchon, G. Daniel, and M.-P. Bouin (2011), Evolution of the seismicity in the eastern Marmara Sea a decade before and after the 17 August 1999 Izmit earthquake, *Tectonophysics*, *510*, 17–27

King, G.C.P., R.S. Stein, and J. Lin (1994), Static stress changes and the triggering of earthquakes, *Bull. Seism. Soc. Am.*, *84*, 935–953

Le Pichon, X., A. M. C. Sengor, E. Demirbag, C. Rangin, C. Imren, R. Armijo, N.

Gorur, N. Cagatay, B. Mercier de Lepinay, B. Meyer, R. Saatcilar, and B. Tok (2001), *Earth Plan. Sc. Letters*, *192*, 595–616

Ma, K.F., C.H. Chan, and R.S. Stein (2005), Response of seismicity to Coulomb stress triggers and shadows of the 1999 Mw=7.6 Chi-Chi, Taiwan, earthquake, *J. Geophys. Res.*, *110*, B05S19

Marsan, D. (2003), Triggering of seismicity at short timescales following Californian earthquakes, *J. Geophys. Res.*, *108*(B5), 2266, doi:10.1029/2002JB001946

Marsan, D., and S.S. Nalbant (2005), Methods for measuring seismicity rate changes: A review and a study of how the Mw 7.3 Landers earthquake affected the aftershock sequence of the Mw 6.1 Joshua Tree earthquake, *Pure Appl. Geophys.*, *162*, 1151–1185, doi:10.1007/s00024-004-2665-4

Nalbant, S.S., A. Hubert, and G.C.P. King (1998), Stress coupling between earthquakes in northwest Turkey and the north Agean Sea, *J. Geophys. Res.*, *103*, 24469–24485

Nur, A., and J. R. Booker (1972), Aftershocks caused by pore fluid flow?, *Science*, *175*, 885–887

Örgülü, G., and M. Aktar (2001), Regional moment tensor inverison for strong aftershocks of the August 17, 1999 Izmit earthquake (Mw=7.4),*Geophys. Res. Lett.*, *28*, 371–374

Özalaybey, S., M. Ergin, M. Aktar, C. Tapirdamaz, F. Bimen, and A. Yörük (2002), The 1999 Izmit earthquake sequence in Turkey : seismological and tectonic aspects, *Bull. Seism. Soc. Am.*, *92*, 376–386

Parsons, T., S. Toda, R. S. Stein, A. Barka, and J. H. Dieterich (2000), Heightened odds of large earthquakes near Istanbul: An interaction-based probability calculation,

374 *Science*, *288*

375 Prejean, S.G., D. P. Hill, E. E. Brodsky, S. E. Hough, M. J. S. Johnston, S. D.
376 Malone, D. H. Oppenheimer, A. M. Pitt and K. B. Richards-Dinger (2004), Remotely
377 triggered seismicity on the United States West Coast following the M 7.9 Denali Fault
378 earthquake, *Bull. Seism. Soc. Am.*, *94*, S348–S359

379 Reasenberg, P.A., and R.W. Simpson (1992), Response of regional seismicity to the
380 static stress change produced by the Loma Prieta earthquake, *Science*, *255*, 1687–1690

381 Steacy, S., J. Gomberg, and M. Cocco (2005), Introduction to special section: Stress
382 transfer, earthquake triggering, and time-dependent seismic hazard, *J. Geophys. Res.*,
383 *110*, B05S01

384 Stein, R. S. (1999), The role of stress transfer in earthquake occurrence, *Nature*,
385 *402*,605–609

386 Stein, R.S., and M. Lisowski (1983), The 1979 Homestead Valley earthquake sequence,
387 California: Control of aftershocks and postseismic deformation, *J. Geophys. Res.*, *88*,
388 6477–6490

389 Stein, R.S., G.C.P. King, and J. Lin (1992), Change in failure stress on the southern
390 San Andreas fault system caused by the 1992 magnitude¡= 7.4 Landers earthquake,
391 *Science*, *258*, 1328-1332

392 Stein, R. S., A. A. Barka, and J. H. Dieterich (1997), Progressive failure on the North
393 Anatolian fault since 1939 by earthquake stress triggering, *Geophys. J. Int.*, *128*,
394 594–604

395 Toda, S., R.S. Stein, P.A. Reasenberg, and J.H. Dieterich (1998), Stress transferred
396 by the Mw=6.9 Kobe, Japan, shock: Effect on aftershocks and future earthquake

probabilities, *J. Geophys. Res.*, *103*, 24543–24565

Toksöz, M. N., A. F. Shakal, and A. J. Michael (1979), Space-time migration of earthquakes along the North Anatolian Fault zone and seismic gaps, *Pageoph.*, *117*, 1259–1270

Voisin, C., F. Cotton, and S. Di Carli (2004), A unified model for dynamic and static stress triggering of aftershocks, antishocks, remote seismicity, creep events, and multi-segmented rupture, *J. Geophys. Res.*, *109*, B06304

Figure 1 : Maps of seismic activity in the Cinarcik Basin, eastern Marmara Sea. The inset shows the location of the studied area. The Main branch of the NAF is in red (Izmit rupture in dotted line, Main Marmara Fault in continuous line). The less active Middle Branch of the NAF is in yellow. The boxes show the extent of the zones over which the cumulative numbers of events are displayed. a) Relocated catalog (used to plot the cumulative number of events in the Prince's Islands zone) from 08/17/1999 to 11/05/1999, without any condition on magnitude. Events during the day following the Izmit earthquake are in green. b) Kandilli catalog (used for the Tuzla, Yalova and Gemlik areas) over the period from 1989 to 2009, for the events of magnitude ≥ 2.8. Events during the 10 years preceding the Izmit earthquake are in green.

Figure 2 : a) Cumulative number of events on the Prince's Islands segment of the Main Marmara Fault from August 17 to November 5, 1999, using the relocated catalog. b) Coulomb stress calculated in the middle of this segment (for the receiver coordinates and configuration, see Table 1) for three different friction coefficients ($\mu = 0.4$, $\mu = 0.6$, $\mu = 0.7$).

Figure 3 : a) Cumulative number of events in the Gemlik region for the decade before and the decade after the earthquake. The blue line represents the cumulative number of background earthquakes before the Izmit mainshock, the red one, after the mainshock. The jump in the cumulative number during the year 2007 is due to a M=5.2 earthquake. We consider only the events of magnitude larger than 3. b) Coulomb stress calculated in the middle of the Gemlik cluster (for the receiver coordinates and configuration, see Table 1) for three different friction coefficients ($\mu = 0.4$, $\mu = 0.6$, $\mu = 0.7$).

Figure 4 : a) Cumulative number of events in the Tuzla cluster for the decade before and the decade after the earthquake. We consider the events of magnitude larger than 2.8. To facilitate comparison, the time scale is reversed before the earthquake. b) Coulomb stress calculated in

the middle of the Tuzla cluster (for the receiver coordinates and configuration, see Table 1) for three different friction coefficients ($\mu = 0.4$, $\mu = 0.6$, $\mu = 0.7$).

Figure 5 : a) Cumulative number of events in the Yalova cluster for the decade before and the decade after the earthquake. We consider the events of magnitude larger than 2.8. To facilitate comparison, the time scale is reversed before the earthquake. b) Coulomb stress calculated in the middle of the Yalova cluster (for the receiver coordinates and configuration, see Table 1) for three different friction coefficients ($\mu = 0.4$, $\mu = 0.6$, $\mu = 0.7$).

Figure 6 : Pressure at the Yalova cluster (the configuration of the receiver is the same as in Figure 5b).

Figure 7 : Map of the peak (positive) dynamic Coulomb stress calculated in each zone of interest. The receiver configurations in each zone is given in Table 2. Black dots denote the events of M$\geq$ 2.8 in the day after the earthquake. Green circles show the M $\geq$ 4 events, for the same period. Blue diamonds indicate the locations where the Coulomb stress time histories of Figures 2b-5b are calculated. The dotted lines show the traces of the Izmit rupture and the Main Marmara Fault. The continuous line is the Middle Branch of the NAF. The dashed boxes show the extent of the zones over which the cumulative numbers of events are displayed.

Figure 8 : Map of the static Coulomb stress changes calculated in each zone of interest. These values are inferred from the amplitude of the stress time histories 100s after the start of the earthquake. The seismicity represented is the activity between October 1, and November 5, 1999. The symbols are the same as in Figure 7.

Figure 9 : Map of the static pressure calculated in each zone of interest. These values are inferred from the amplitude of the pressure time histories 100s after the start of the earthquake.

452 The seismicity represented is the activity between October 1, and November 5, 1999. The symbols
453 are the same as in Figure 7.

Table 1. Parameters used for the stress calculation in each cluster. Strike is given from north.

Cluster name	lon (deg.)	lat (deg.)	depth (km)	strike (deg.)	dip (deg.)	rake (deg.)
Prince's Islands	29.07	40.79	10	113	90	0
Gemlik	29.16	40.43	10	90	90	0
Yalova	29.10	40.63	10	300	60	90
Tuzla	29.19	40.76	10	155	70	90

Table 2. Parameters used for the calculation of stresses in each area

Zone	lon. min. (deg.)	lon. max. (deg.)	lat. min. (deg.)	lat. max (deg.)	strike (deg.)	dip (deg.)	rake (deg.)
1	29.01	29.13	40.77	40.82	113	90	0
2	28.16	29.33	40.27	40.52	90	90	0
3	29.15	29.27	40.73	40.80	155	70	90
4	28.84	29.26	40.52	40.66	300	60	90
5	28.60	28.89	40.83	40.93	105	78	0
6	28.89	29.01	40.77	40.93	113	90	0
7	29.33	29.70	40.27	40.52	90	90	0

Supplementary Figure S1 : Map of the peak (positive) dynamic Coulomb stress calculated in each zone of interest. The receiver configurations are the same as for figure 7, except that for zones 2 and 7, we consider normal faulting mechanism instead of a strike-slip one. Black dots denote the events of M$\geq$ 2.8 in the day after the earthquake. Green circles show the M$\geq$ 4 events, for the same period.

Supplementary Figure S2 : Map of the static Coulomb stress changes calculated in each zone of interest. The receiver configurations are the same as for figure 8, except that for zones 2 and 7, we consider normal faulting mechanism instead of a strike-slip one. The seismicity represented is the activity between October 1, and November 5, 1999. The symbols are the same as in Supplementary Figure S1.

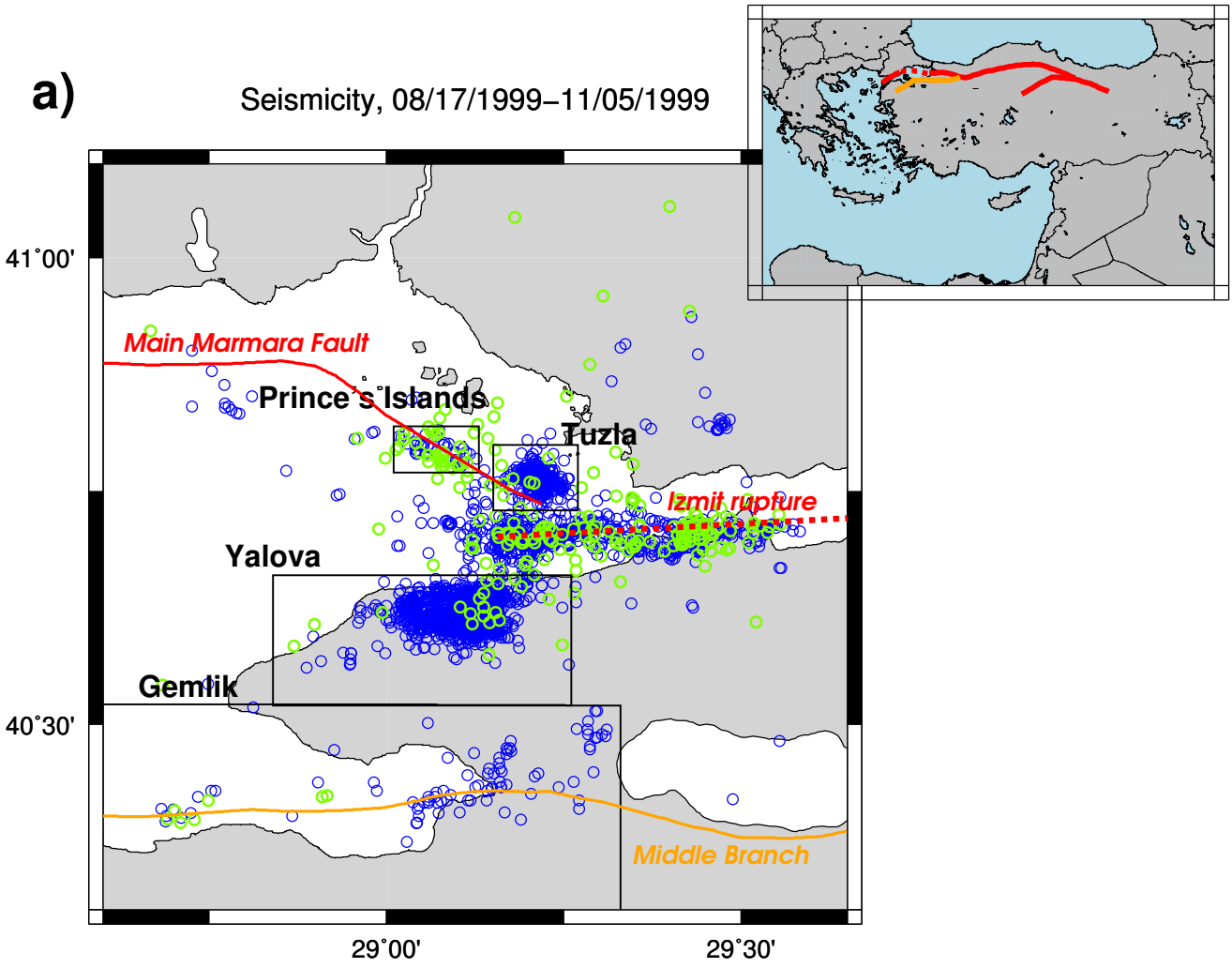
a)
Seismicity, 08/17/1999–11/05/1999
41°00'
40°30'
29°00'
29°30'
Main Marmara Fault
Prince's Islands
Tuzla
Izmit rupture
Yalova
Gemlik
Middle Branch

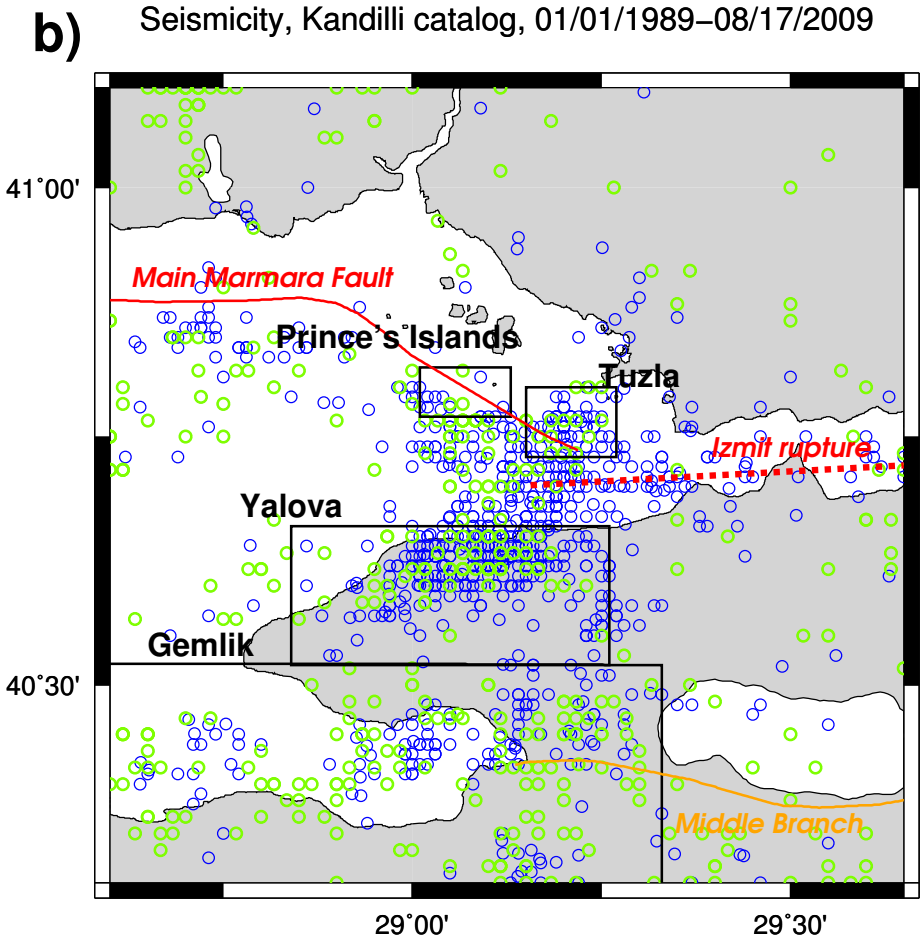
b)
Seismicity, Kandilli catalog, 01/01/1989–08/17/2009
41°00'
40°30'
29°00'
29°30'
Main Marmara Fault
Prince's Islands
Tuzla
Izmit rupture
Yalova
Gemlik
Middle Branch

Figure 1

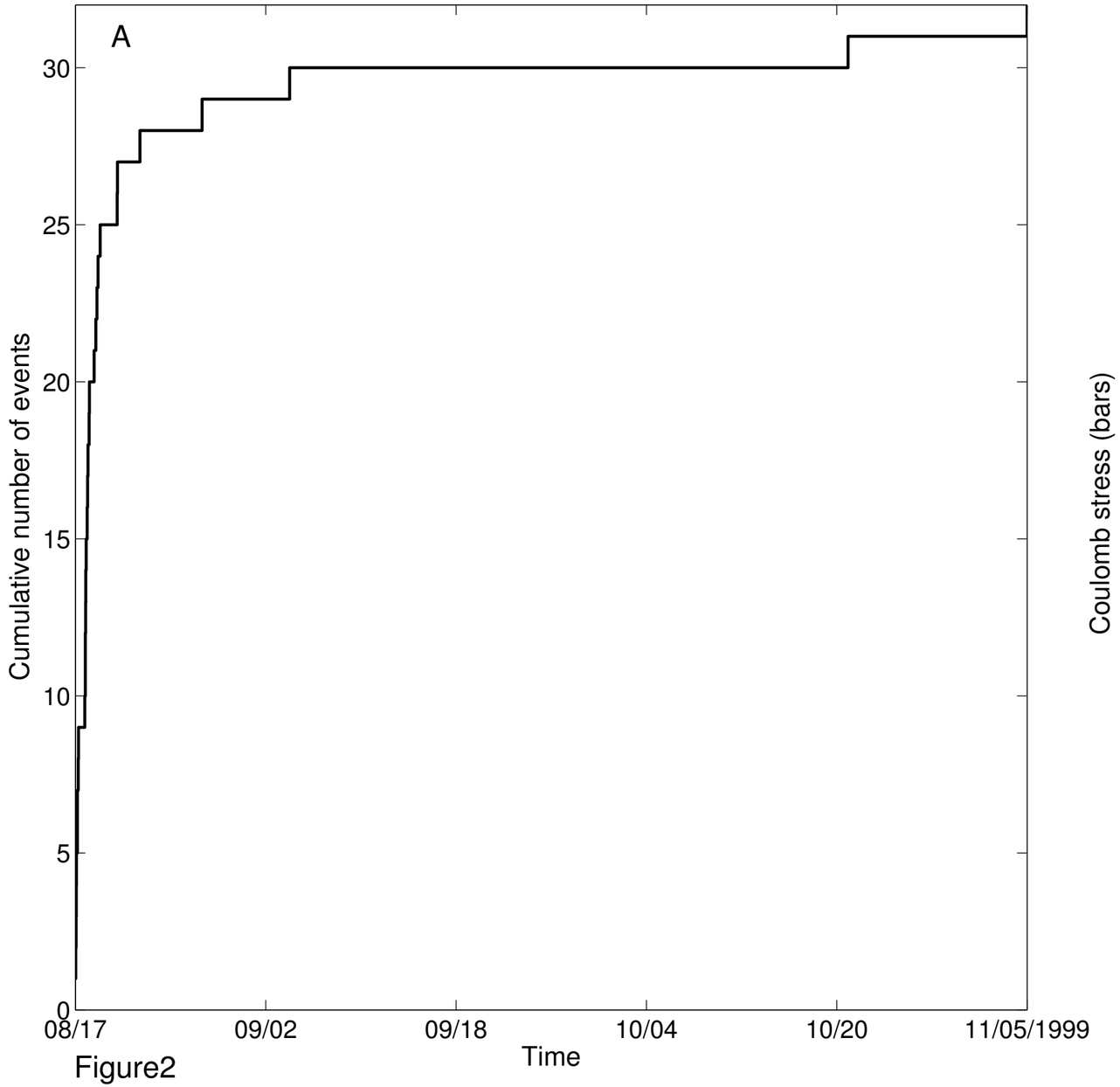
A
Cumulative number of events
0
5
10
15
20
25
30
08/17
09/02
09/18
10/04
10/20
11/05/1999
Time

Figure2

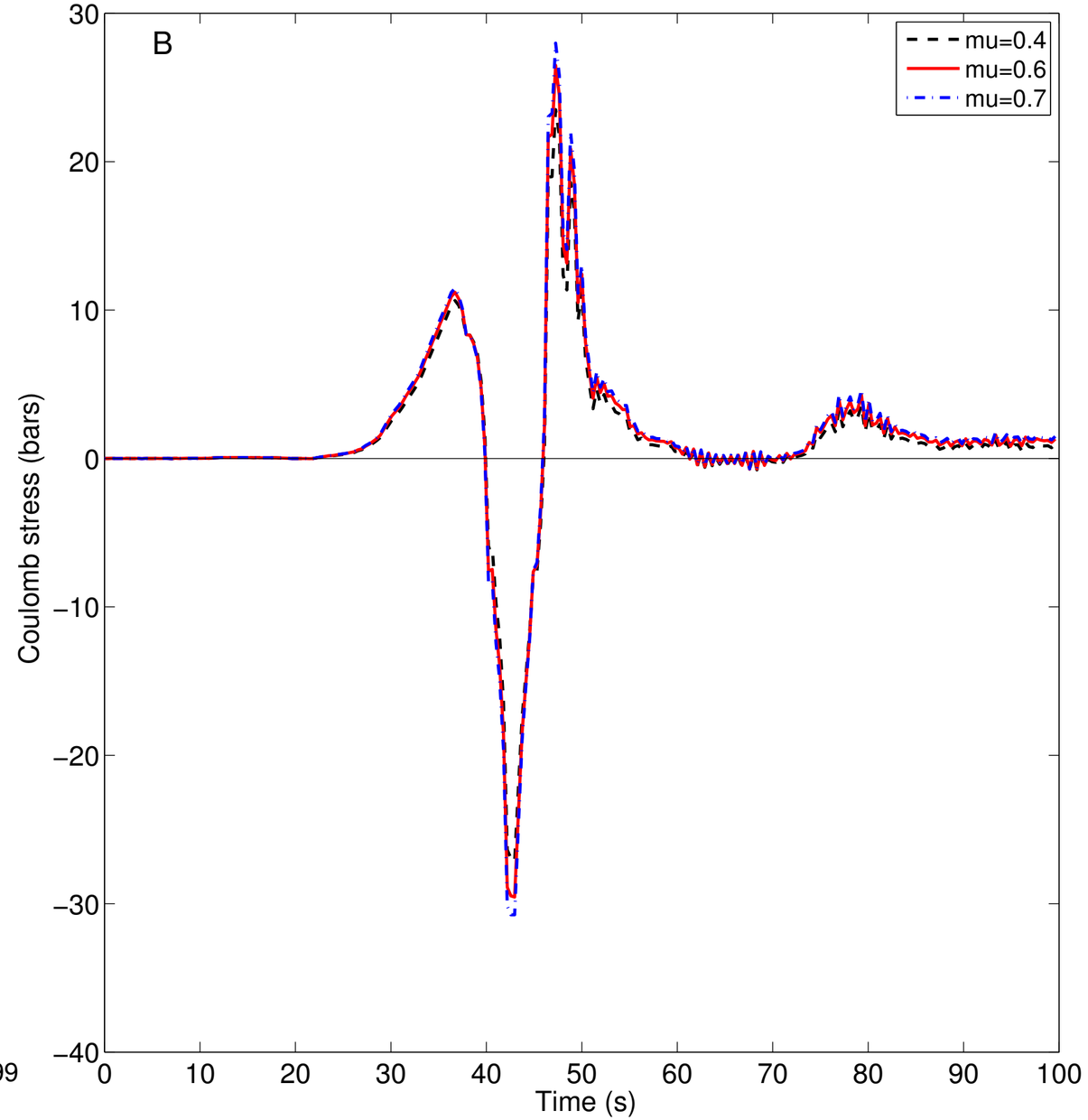
B
mu=0.4
mu=0.6
mu=0.7
Coulomb stress (bars)
30
20
10
0
−10
−20
−30
−40
0
10
20
30
40
50
60
70
80
90
100
Time (s)

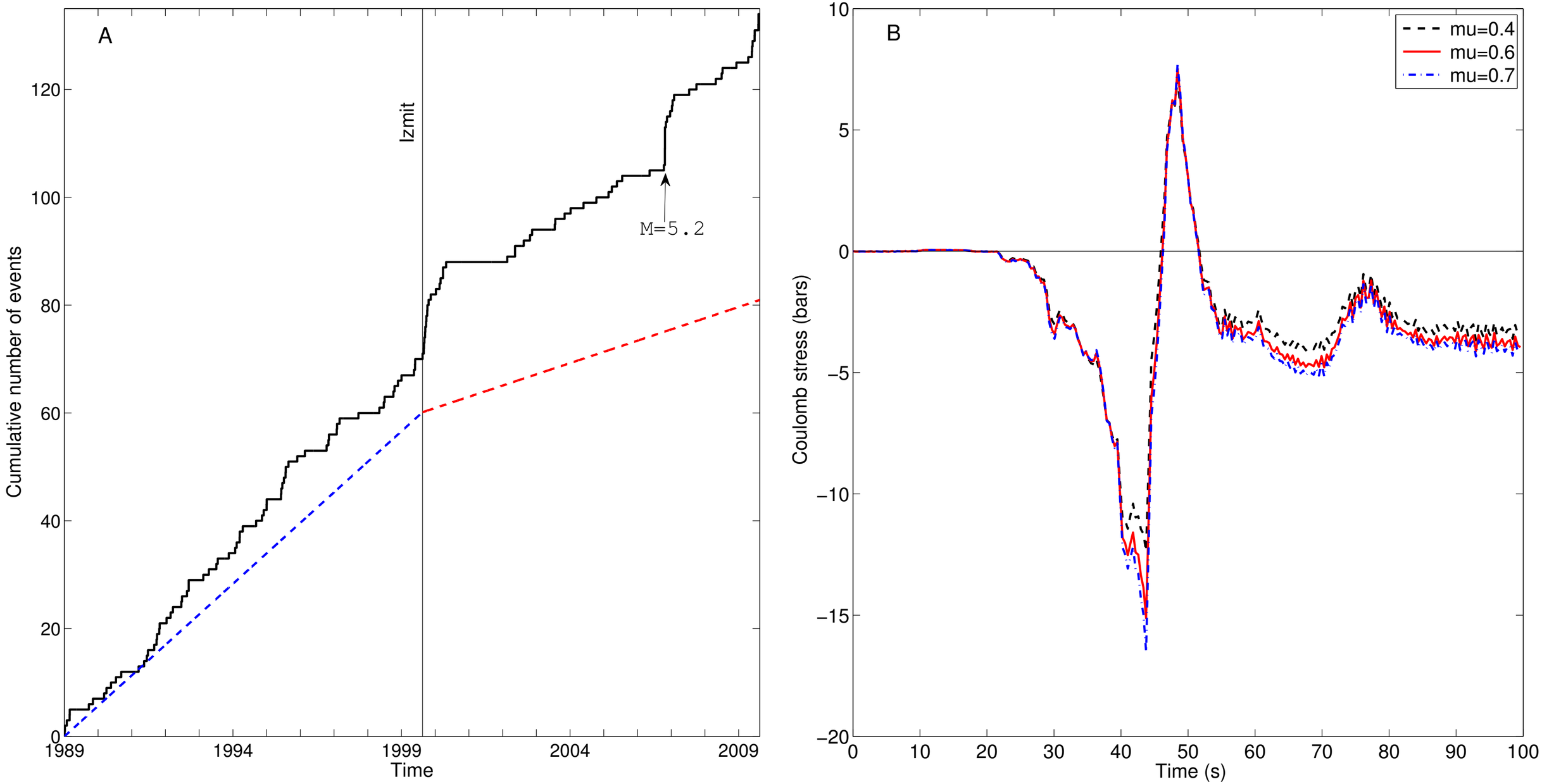
A
Izmit
M=5.2
Cumulative number of events
Time
0
20
40
60
80
100
120
1989
1994
1999
2004
2009
B
mu=0.4
mu=0.6
mu=0.7
Coulomb stress (bars)
Time (s)
10
5
0
−5
−10
−15
−20
0
10
20
30
40
50
60
70
80
90
100

Figure 3

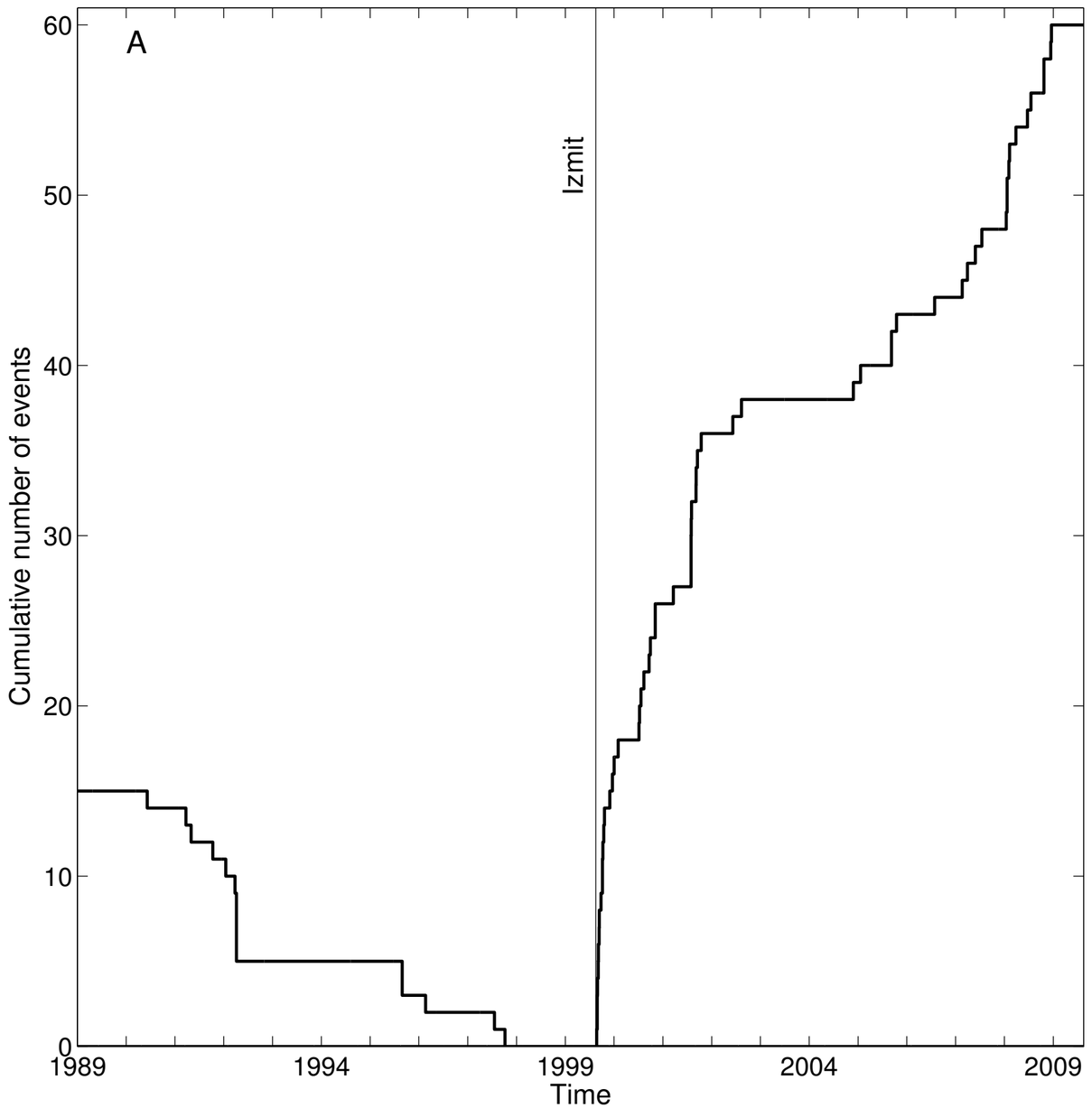
A
Izmit
Cumulative number of events
Time
0
10
20
30
40
50
60
1989
1994
1999
2004
2009

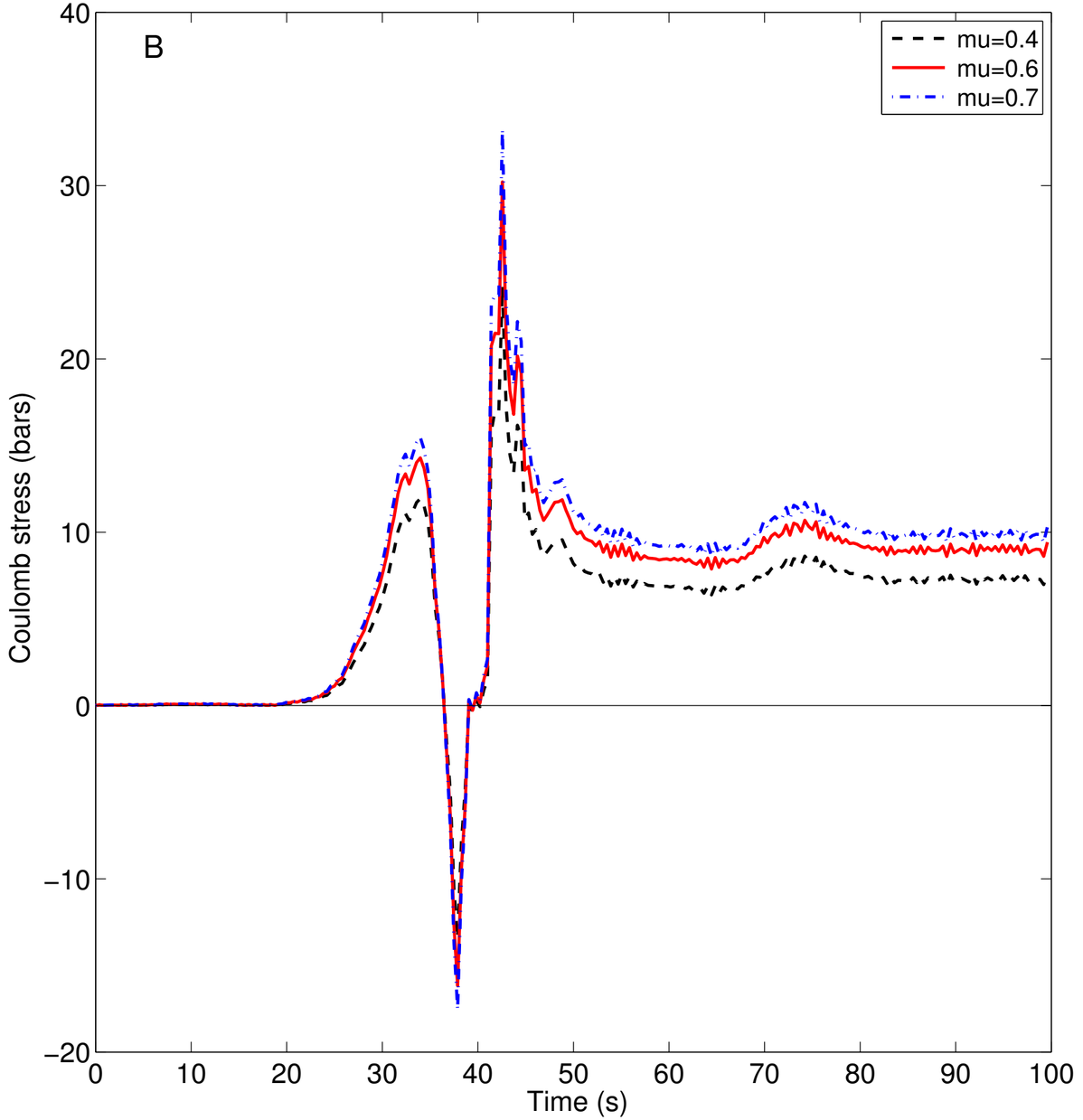
B
mu=0.4
mu=0.6
mu=0.7
Coulomb stress (bars)
Time (s)
40
30
20
10
0
−10
−20
0
10
20
30
40
50
60
70
80
90
100

Figure 4

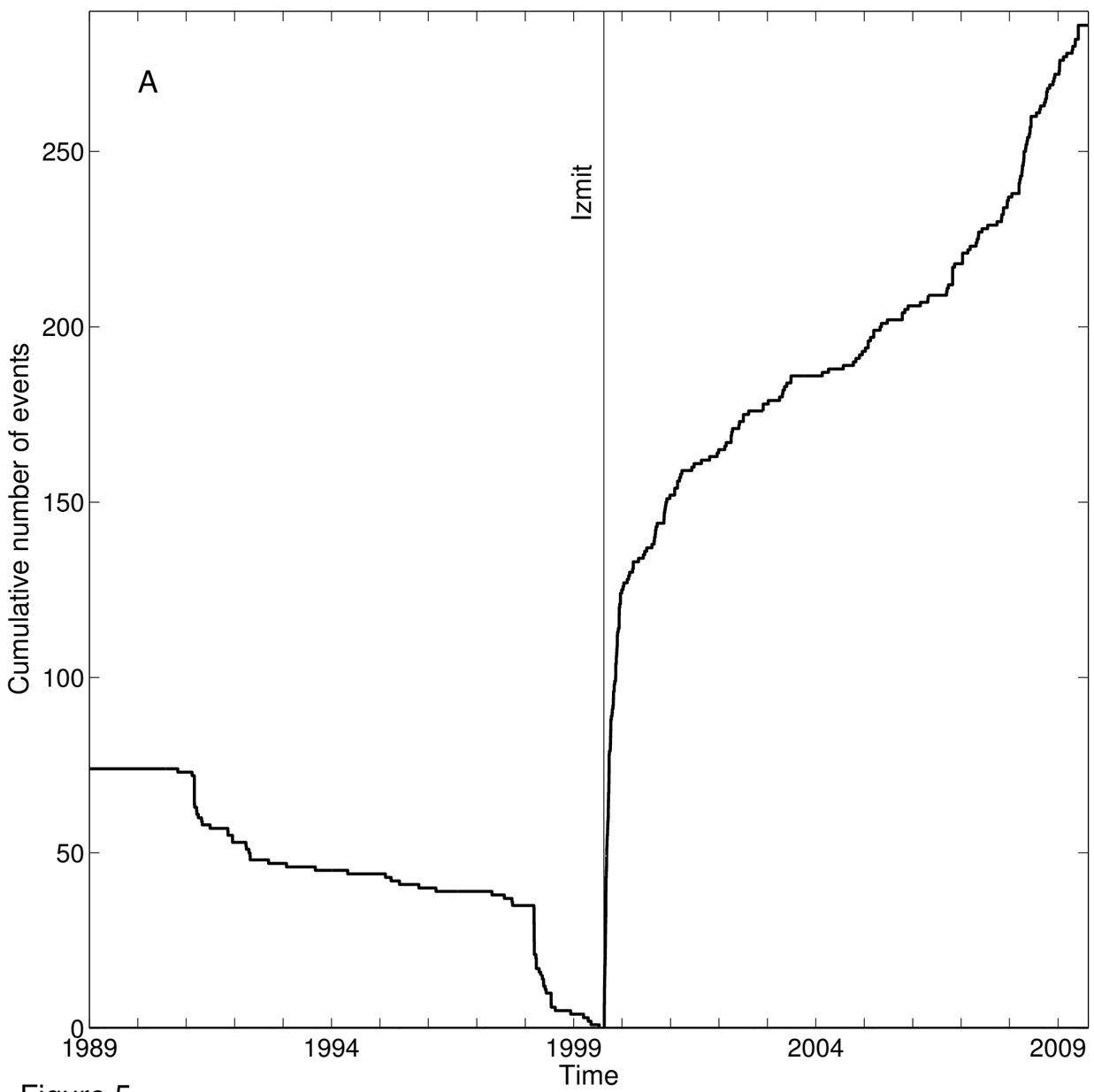
A
Izmit
Cumulative number of events
Time
0
50
100
150
200
250
1989
1994
1999
2004
2009

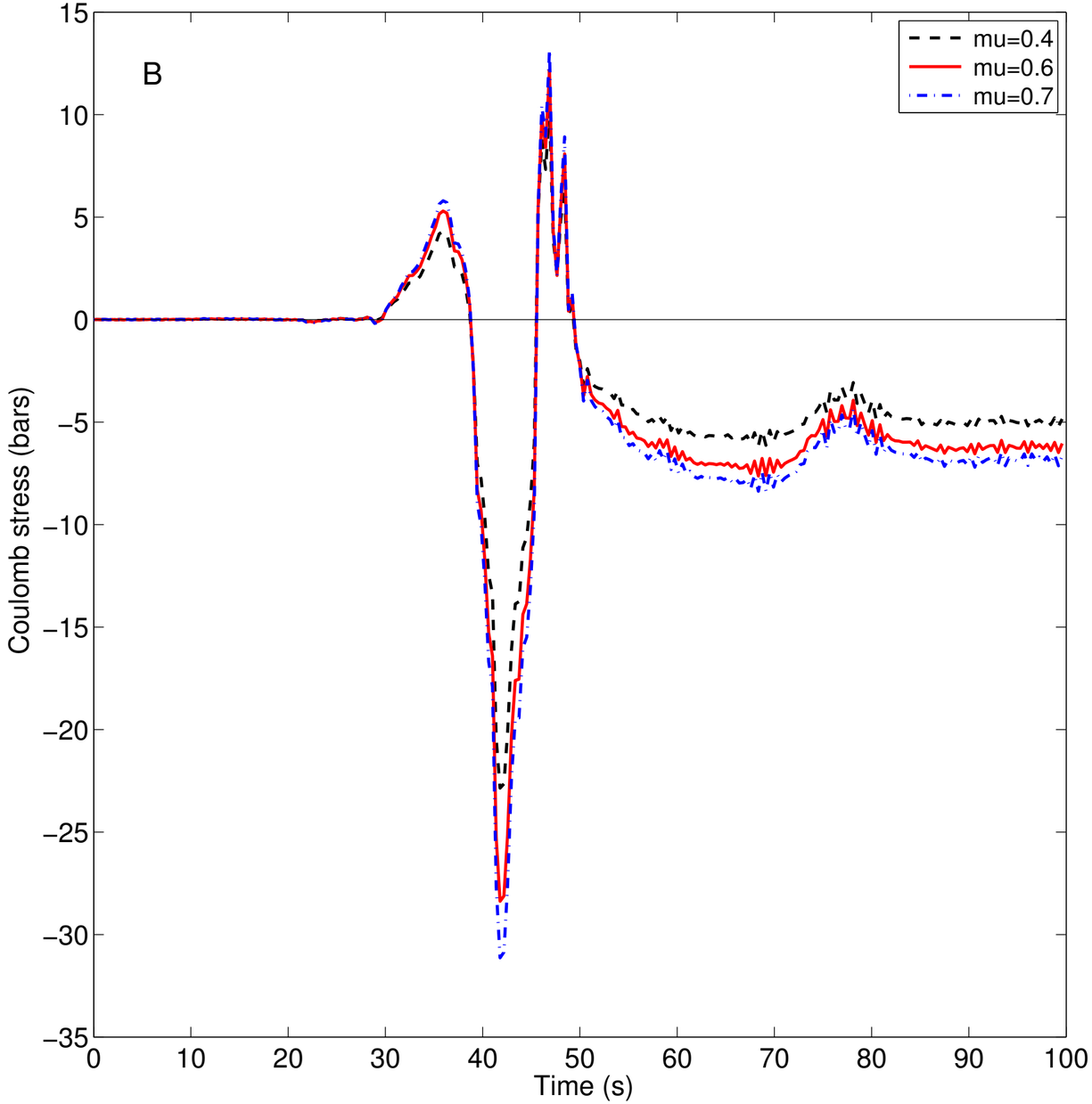
B
mu=0.4
mu=0.6
mu=0.7
Coulomb stress (bars)
Time (s)
15
10
5
0
−5
−10
−15
−20
−25
−30
−35
0
10
20
30
40
50
60
70
80
90
100

Figure 5

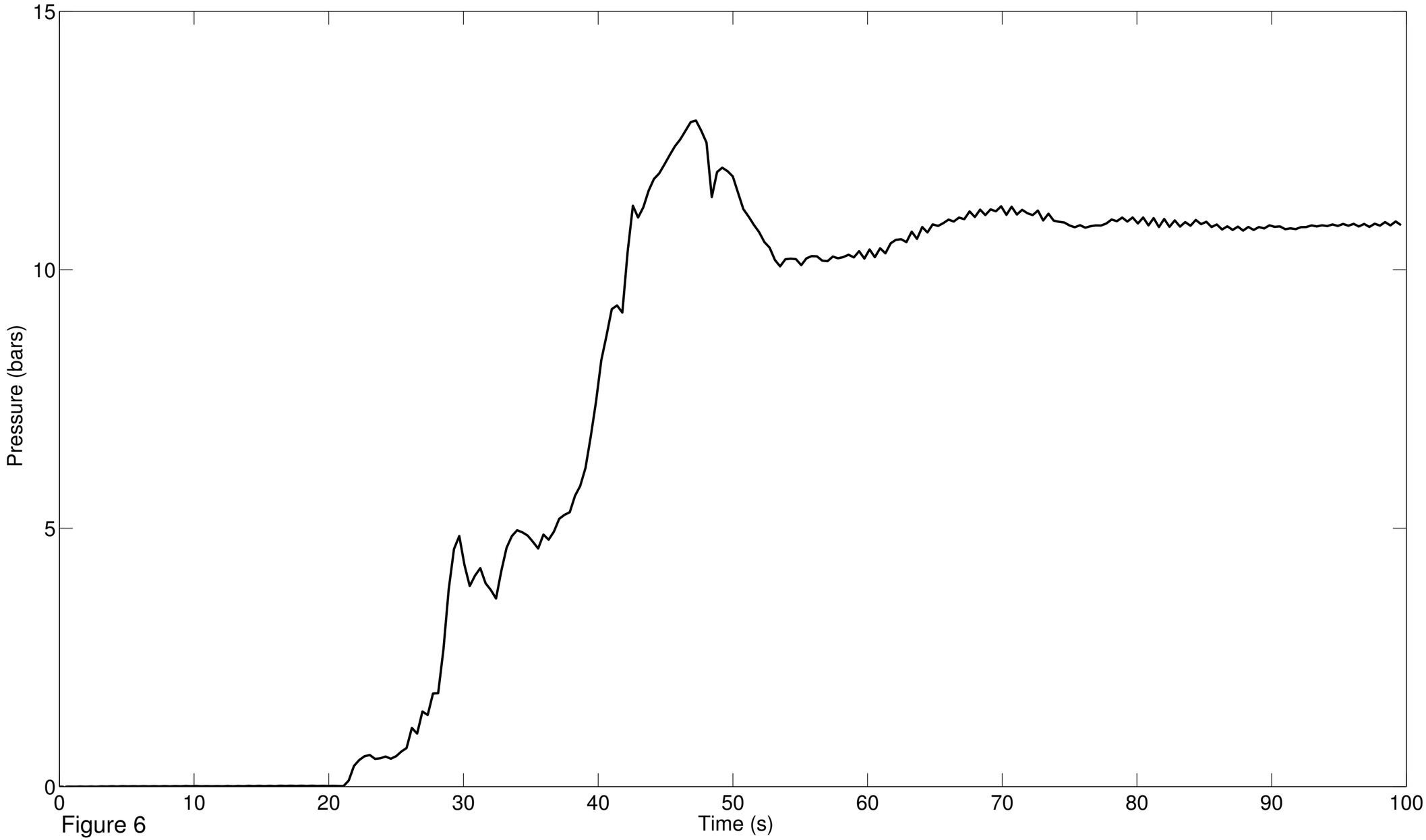

Figure 6

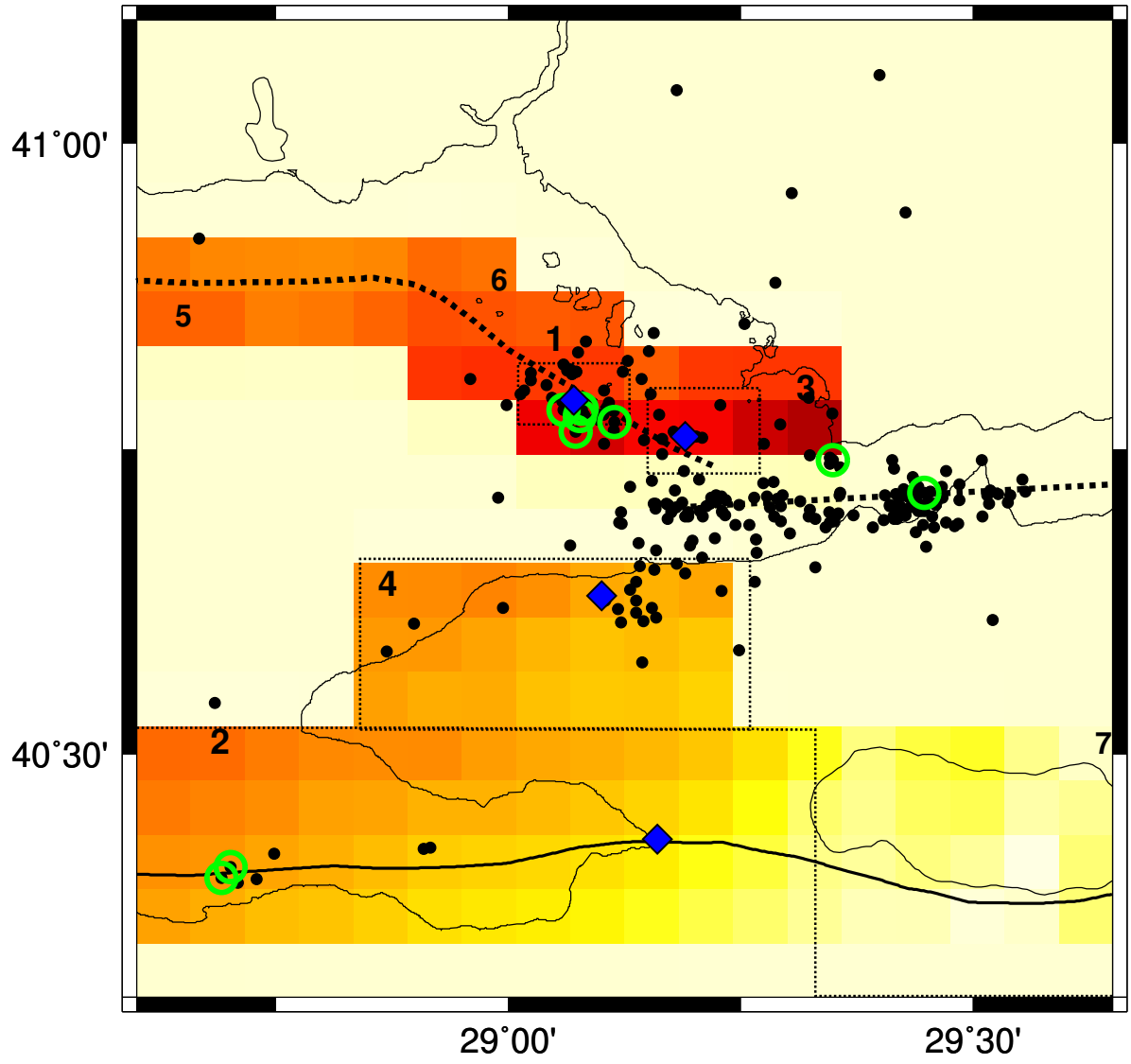

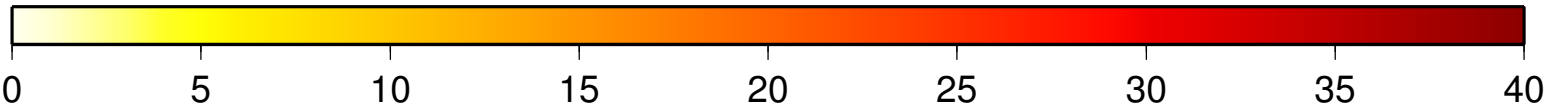

dynamic Coulomb stress

Figure 7

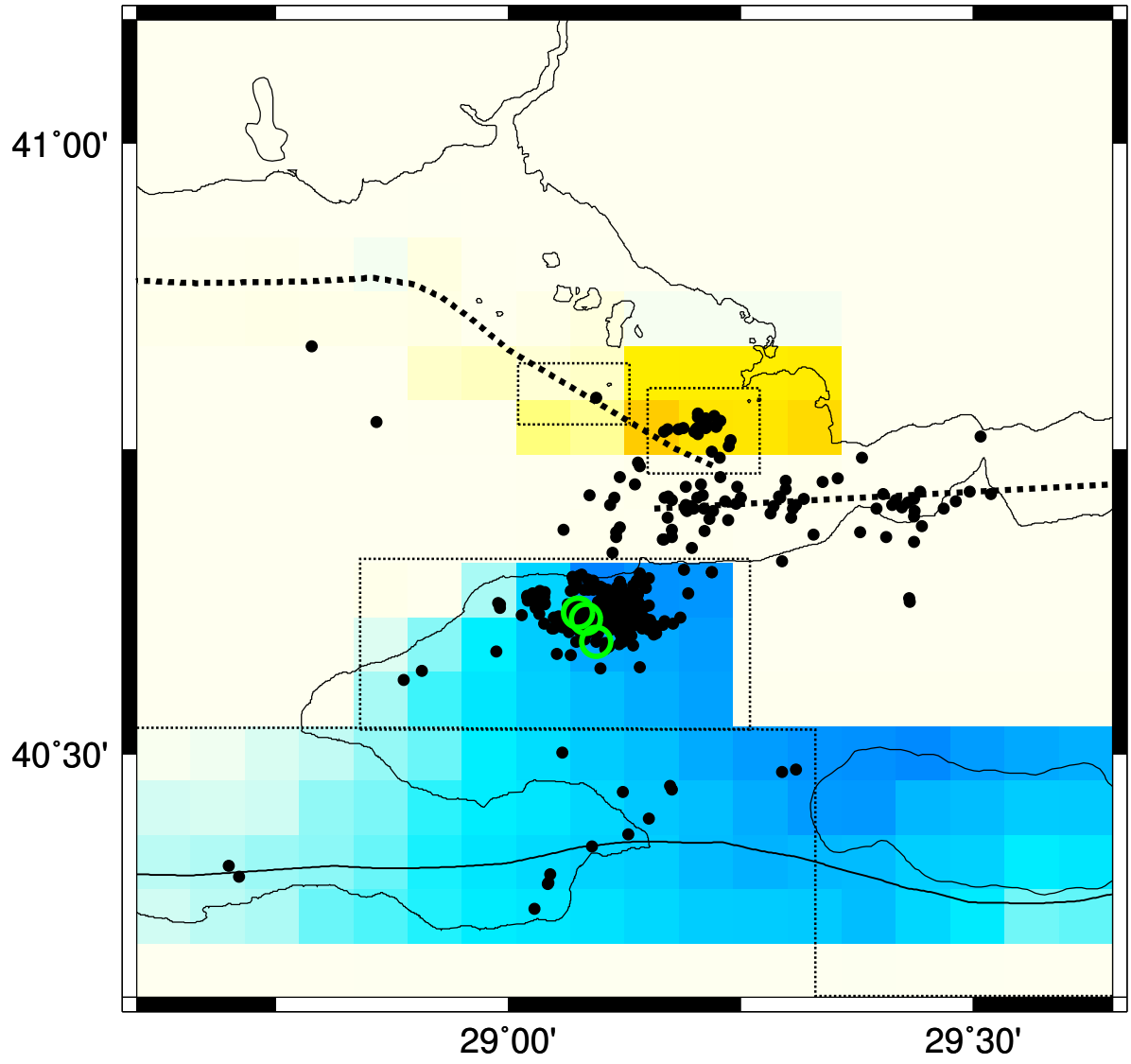

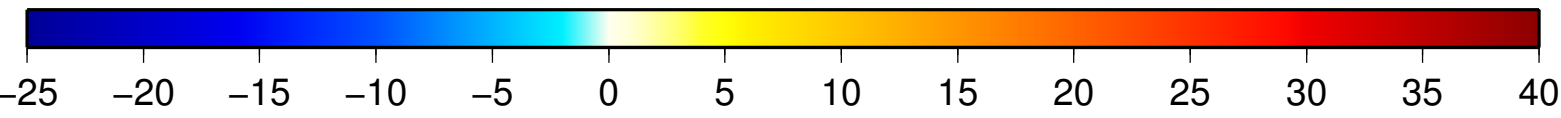

static Coulomb stress

Figure 8

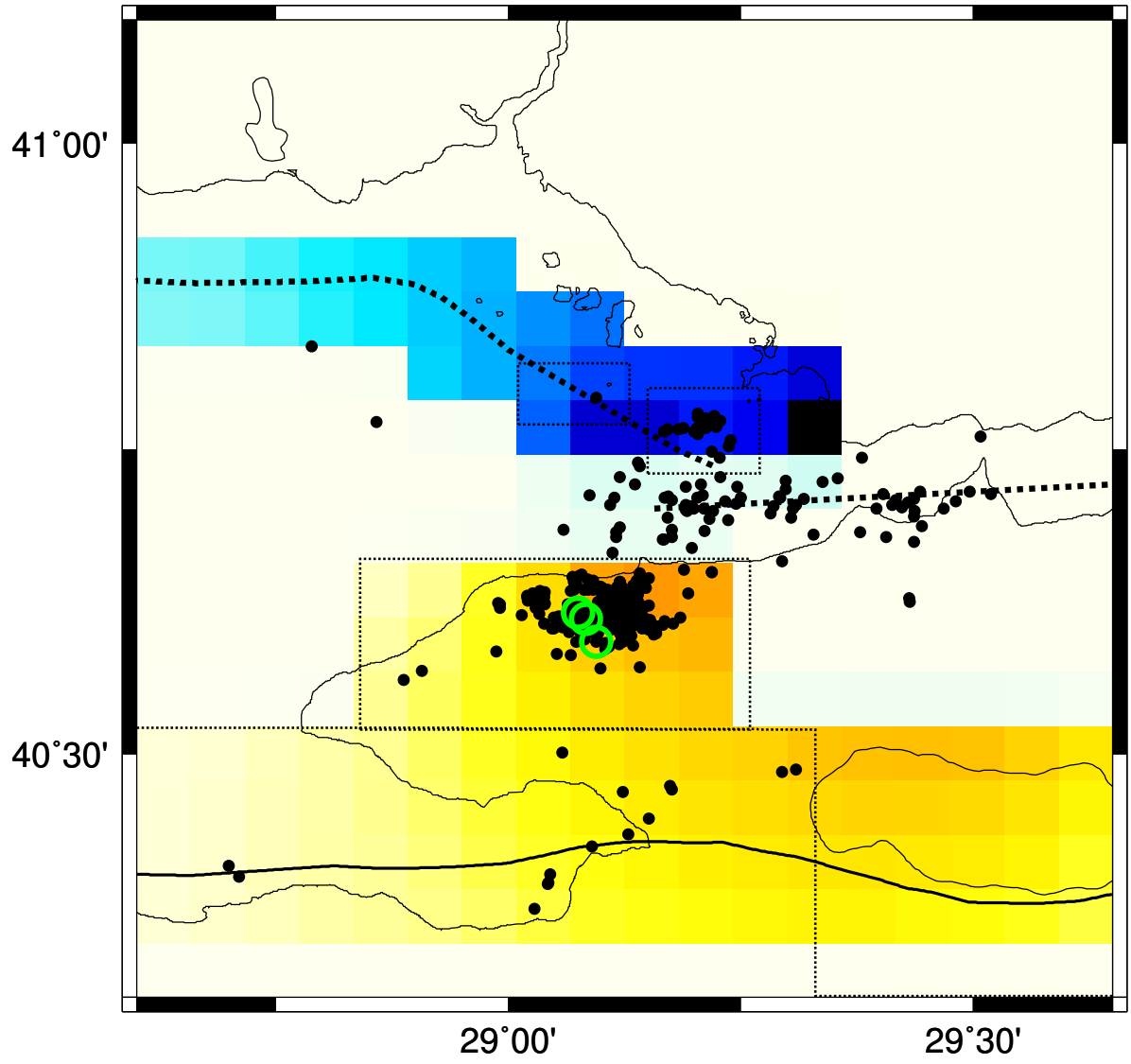

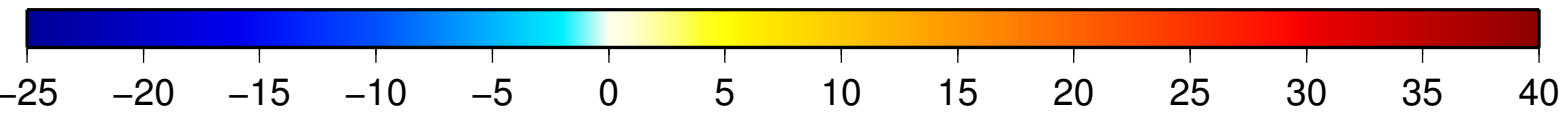

static Coulomb pressure

Figure 9